Inclination Angles Effect on Heat Transfer and Turbulent Periodic Flow in a Duct-Mounted Flow-Inclined Baffles

Kamil Arslan[1] · Recep Ekiciler[2] · Nevzat Onur[2]

Abstract

This research uses computational methods to examine steady-state turbulent forced convection flow in a duct having rectangular cross-section equipped with flow-inclined baffles on the bottom wall. The aim of this study is to provide information about turbulent convective heat transfer in ducts with a roughened surface. Especially, it is intended to obtain the influence of newly designed baffles on convective heat transfer in detail. Between 1000 and 10,000, the Reynolds number is varied. The duct's hydraulic diameter is 75 mm. Air is used as the working fluid. Numerical calculations have been carried out using *Ansys Fluent R18* commercial code. Governing equations have been solved iteratively. *SST k-ω* turbulence model has been used for solving turbulence equation. New engineering correlations have been gained from numerical calculations. In terms of the thermal enhancement factor, a number of different baffle inclination angles have been evaluated in comparison with both one another and a smooth duct. The results show that a steeper inclination angle of the baffle improves the heat transmission. Pressure drop also rises as the baffle inclination angles become steeper. In all situations, the greatest thermal augmentation factor is obtained at an inclination angle of $\beta = 0.41$ rad, while the least is obtained at an inclination angle of $\beta = 0$ rad.

Keywords Periodic flow · Inclination angle · Turbulent flow · Passive techniques · Heat transfer enhancement · Baffle

List of Symbols

$\dot{Q}$ Convective heat transfer (W)
A Surface area (m^2)
c_p Specific heat (J/kg K)
f Darcy friction factor (−)
Pr   Prandtl number (−)
L Length of the duct (m)
k Thermal conductivity (W/m K)
Nu   Nusselt number (−)
h Heat transfer coefficient (W/m^2 K)
T Temperature (K)
U Velocity (m/s)
Re Reynolds number (−)
k Thermal conductivity (W/m K)
β Inclination angle of baffle (rad)

Θ Dimensionless temperature (−)
ρ Density (kg/m^3)

Subscripts

b Bulk
c Cross-sectional
i Inlet
o Outlet, smooth
w Wall

✉ Recep Ekiciler
   recepekiciler@gazi.edu.tr

[1] Department of Mechanical Engineering, Faculty of Engineering, Karabük University, 78050 Karabük, Turkey

[2] Department of Mechanical Engineering, Faculty of Engineering, Gazi University, 06570 Ankara, Turkey

1 Introduction

Several methods have been used to improve heat transmission in several manufacturing processes; they include active, passive, and hybrid approaches. Passive techniques are commonly used in comparison with active techniques due to the simple manufacturing process. Ribs, dimples, twisted tapes, baffles, etc., are inserted in the flow region as inserts to boost heat transfer. Passive approaches play a crucial role

in heat exchanger construction because they alter the local heat transfer coefficient and flow field, leading to improved heat transfer rate and lower pressure drop.

Researchers have been investigating on the impact of ribs, baffles, and twisted tape on flow characteristics and heat transfer in heat exchanger ducts for decades. For their researches, Dutta and Dutta [1] used a rectangular duct with a variety of different-sized and positioned inclined baffles. Various baffles, both perforated and solid, are attached to the duct. They looked for the duct's best possible heat transfer configuration. Salem et al. [2] analyzed the influence of parameters of baffle characteristics such as open area ratio, hole spacing ratio, and inclination angles in heat exchangers having a double pipe with an experimental study. The presence of a multi-V-perforated baffle in a rectangular duct was tested experimentally by Kumar et al. [3]. They examined how changing the baffle's relative width (from 1 to 6) affected the heat transfer. They found that heat transfer magnitude reaches the highest value at the relative width of the baffle is 5. Experimental research on the heat transfer characteristics of turbulent flow in a duct featuring inclined and transverse twisted baffles on the bottom surface was conducted by Eiamsa-ard et al. [4]. A comparison was made between transverse and angled baffles, with the emphasis being on the physical parameters. The horseshoe baffle, with its variable pitch and height, was studied numerically and experimentally by Skullong et al. [5] to determine its ideal placement in a square duct heat exchanger. They noticed that the smallest relative pitch and the biggest relative height of the baffle show the best thermal performance. Qayoum and Panigrahi [6] investigated the thermal performance of smooth, split slit-ribbed, slit-ribbed, and solid-ribbed square ducts for turbulent flow conditions. It was observed that split-ribbed presents better heat transfer augmentation. Wang et al. [7] looked at how heat exchangers' thermal capacity changed depending on the plate spacing and hole height of perforated baffles with four blades. According to their findings, reducing the plate hole height and spacing increases the pressure drop and the heat transfer coefficient while lowering the heat transfer coefficient per unit pressure losses. Experiments were conducted by Ko and Annand [8] within a rectangular duct with porous baffles attached to the upper and lower walls. The results of the experiments were endorsed by the literature. The duct-mounted porous baffle produced heat transfer augmentation of 300% in comparison with the duct having no baffle. Jadsadaratanachai et al. [9] performed a numerical simulation in a circular duct-mounted 45°V-baffle for determining flow and heat transfer features under laminar flow conditions. They investigated the influence of the blockage ratio in this study. According to Promvonge [10], a square duct fitted with 30°V-fins and counter-twisted tape improves heat transmission and flow characteristics. The numerical investigation by Sripattanapipat and Promvonge

[11] was conducted in a diamond-shaped and flat-baffled two-dimensional duct. Using two-waisted triangular baffles in a rectangular duct, Menni et al. [12] demonstrated the heat transfer and flow properties of this configuration. It was released that the variation of friction loss and Nusselt number (Nu) were the largest near the baffles resulting from a powerful velocity gradient. Promvonge and Thianpong [13] experimentally conducted a study to understand the effect of the shape of the rib on heat and flow features in channels exposed to constant heat flux on the surfaces. Three configurations of rib shapes (triangular, wedge, and rectangular) were utilized for testing. They reached that the triangular shape of the rib shows the best performance. Kelkar and Patankar [14] carried out two-dimensional numerical simulations of finned passages composed of two plates according to heat transfer. They studied the effects of parameters of Reynolds number, geometric variation of fin, and fin-conductance. It was noticed that the flow is substantially directed and intruded to the other plate and this phenomenon enhances the heat transfer. To address the turbulent flow in a square duct, Kamali and Binesh [15] created a computer code with four possible rib forms, including triangles, squares, trapezoids, and varying heights for the flow route. The outcomes exhibited that the optimal thermal performance is achieved by a trapezoidal rib design with diminishing height. The heat transfer research of turbulent flow in square duct-mounted V-baffles was also performed by Fawaz et al. [16]. The air was selected for working fluid. Influences of pitch and blockage ratio of baffles on heat transfer features were inspected. They get the result that the Nu increases with a higher blockage ratio and lower pitch ratio. Debnath and Pradhan [17] studied review of the literature on heat transfer enhancement characteristics and material selection of shell and coil tube heat exchangers. The effect of increasing convective heat transport on the fluid–solid interface of a helical coil was studied. It was proposed that the convective heat transfer rate and the material selection for low-cost manufacturing with minimal dimensions may both be improved with the help of some novel concepts. The influence of heat transfer and chemical reaction on laminar fluid flow in a channel with several obstructions was studied numerically by Masud et al. [18]. COMSOL multi-physics software was used for numerical simulation. The results showed that water breakdown is more pronounced around circular objects. When the ratio of obstacle spacing increases, thermal breakdown of the fluid decreases. Ibrahim et al. [19] performed a study that used a two-phase model to examine the heat transfer rate and flow of non-Newtonian water-carboxyl methyl cellulose-based Al_2O_3 nanofluid in a helical heat exchanger fitted with conventional and unique turbulators. This research finds that replacing a basic smooth system with a unique heat exchanger improves thermal characteristics by approximately 210%, decreases hydraulic performance by about

28%, and boosts the performance assessment criterion index by about 57%. Based on the first and second principles of thermodynamics with varying geometries, Ibrahim et al. [20] conducted a numerical study that evaluated the forced convection of nanofluid flow within a circular microtube with twisted porous blocks in the presence of a uniform magnetic field. In addition, further information can be obtained from Refs. [16, 21–26].

To the author's knowledge, and based on a survey of the relevant literature, the thermal and hydrodynamic aspects of flow in a duct having rectangular cross-section with baffles having trapezoid-shaped at the bottom wall at varying inclination angles have not been studied numerically under turbulent flow condition, despite their relevance to a wide range of thermal applications. The trapezoid-shaped baffle is examined to see how its unique fabrication of the flow and heat transfer properties in the periodically developed regime. The goal of this study is to provide information about turbulent convective heat transfer in ducts with a roughened surface and a rectangular cross-section. The new-designed baffles have been used for obtaining higher convection heat transfer rates with lower pumping power requirements. This phenomenon will also give fabricating more efficient or smaller heat exchangers in the future. The flow chart of the study is exhibited in Fig. 1.

2 Material and Methodology

The dimensions of the baffle, which is positioned on the duct's bottom and is formed like a trapezoid, are shown in Fig. 2. The influence of the inclination angle of the baffle (β) and flow condition is the primary focus of this investigation. The greater the baffle inclination angle, the more noticeably the flow resistance increases. A large baffle inclination angle forces the most fluid to flow to the bottom wall, so this condition increases the convective heat transfer in this region. The baffle inclination angle has to be adjusted such that the heat transmission and flow resistance are both minimized. Obtaining the optimum baffle inclination angle is the aim of his study.

On the test duct's base plate, the flow-inclining baffles have been spaced 15 mm apart in three arrays. Changing the baffle's downstream height by 4.5-, 6.0-, 7.5-, or 9.0 mm results in $\beta = 0.41$ rad, 0.28 rad, 0.14 rad, and 0 rad, respectively, controlling the baffle's angular position. The front baffle height has been kept constant at 9.0 mm. The baffles are installed in the duct's base plate. The bottom baffled duct surface is kept at uniform temperature conditions.

In this research, a duct with a rectangular cross-section and baffles installed on its bottom are modeled mathematically for using in three-dimensional numerical simulations. The working fluid is air. The 3D steady-state Newtonian incompressible flow with negligible buoyancy effects and viscous dissipation are marked as turbulent. It is supposed that the thermophysical characteristics of air remain unchanged with temperature. According to research done by Sparrow and Tao [27], in a channel that is subject to periodic disturbances, the fluid flow may reach a periodically fully developed regime within just a few cycles from the channel's entry. In this regime, the mean heat transfer rates and the pressure drops for each cycle are identical. Therefore, periodically fully developed regime is assumed in this study and, only the periodic region is investigated in the numerical investigation (Fig. 3a). The results of the experimental investigation that Arslan and Onur [28] conducted provided the basis for determining the size of the computational domains. Due to the symmetry that exists between the axis plane and the flow field, only one-half of the area has been taken into consideration for the computational domain. The x-axis describes the main direction of motion.

A schematic diagram and the grid distribution of the computational geometry are given in Fig. 3b. In the current investigation, tetrahedral grids are constructed. Close to duct and baffle surfaces, the number of grids is increased to improve the accuracy and resolution.

Simulations are run to examine the transition to the turbulent zones. Radiation effects are neglected in the solution of the energy equation. *Shear-Stress Transport (SST) k-ω* turbulence model is used in the calculations. To calculate the energy and Reynolds averaged Navier–Stokes equations for turbulent flow, numerical analysis is combined with transport equation analysis. In all of the computations, the average y^+ value was chosen to be quite close to 1.0, which is sufficient for adequately resolving the laminar sublayer.

In the process of doing the numerical computations, the equations pertaining to momentum, continuity, energy, and turbulence are all solved. In light of this, the equations of continuity, momentum, and energy, as well as the *SST k-ω* turbulence model, can be described as follows [29]:

Continuity Equation:

$$\frac{\partial \overline{u}_j}{\partial x_j} = 0 \tag{1}$$

Momentum Equation:

$$\frac{\partial}{\partial x_j}(\overline{u}_i \overline{u}_j) = f_i - \frac{1}{\rho}\frac{\partial \overline{p}}{\partial x_i} + \frac{\partial}{\partial x_j}\left[\frac{\mu}{\rho}\left(\frac{\partial \overline{u}_i}{\partial x_j} + \frac{\partial \overline{u}_j}{\partial x_i}\right)\right]$$
$$+ \frac{1}{\rho}\frac{\partial}{\partial x_j}(-\rho \overline{u'_i u'_j}) \tag{2}$$

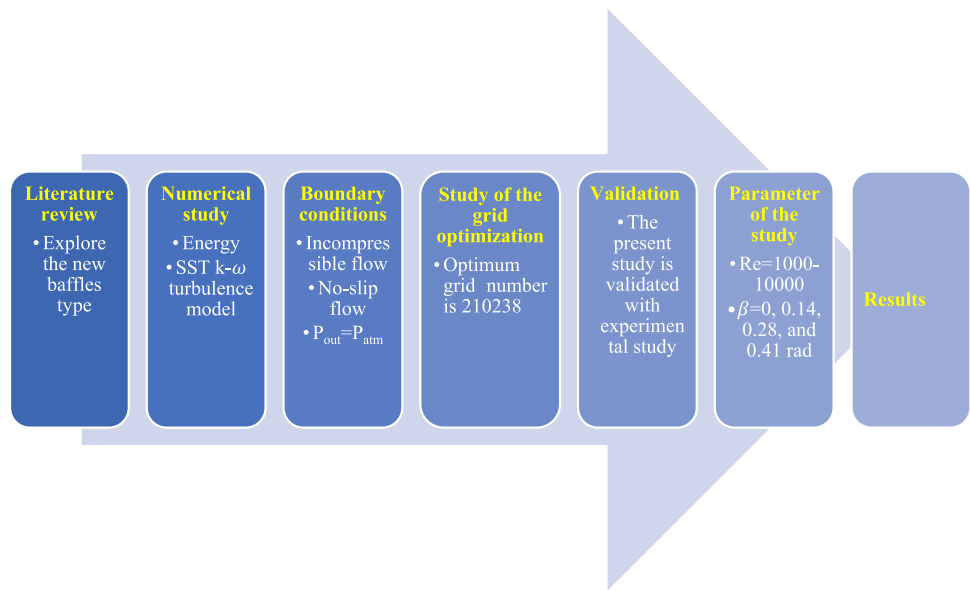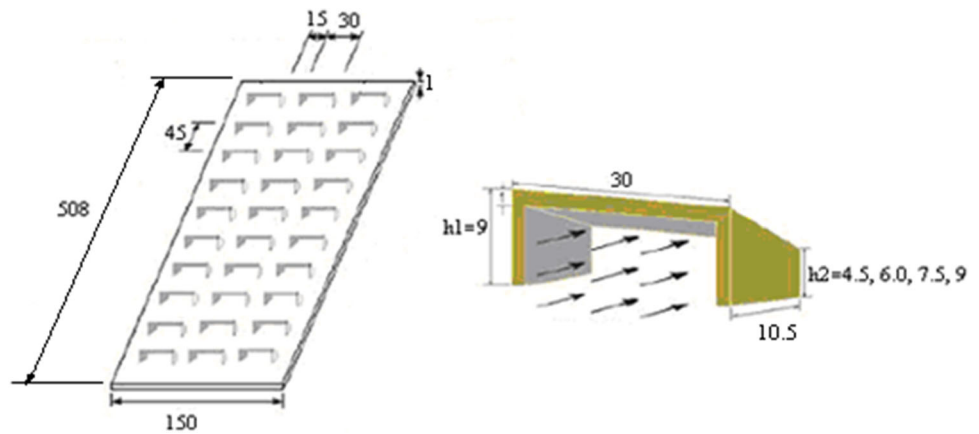**Fig. 1** Flow diagram of the study

Fig. 2 Sketch of the trapezoid-shaped baffle and its dimensions (dimensions are mm)

Energy Equation:

$$\frac{\partial}{\partial x_j}(\overline{u}_j \overline{T}) = \frac{\partial}{\partial x_j}\left[\alpha\left(\frac{\partial \overline{T}}{\partial x_j}\right)\right]$$

$$+ \frac{1}{\rho c_p}\frac{\partial}{\partial x_j}(-\rho c_p \overline{u'_{jj} T'}) + \frac{v}{c_p}\overline{\Phi}_v + \frac{u'''}{\rho c_p} \quad (3)$$

$$\overline{\Phi}_v = \left(\frac{\partial \overline{u}_i}{\partial x_j} + \frac{\partial \overline{u}_j}{\partial x_i} + \delta_{ij}\right)\frac{\partial \overline{u}_i}{\partial x_j} + \left(\frac{\partial u'_i}{\partial x_j} + \frac{\partial u'_j}{\partial x_i} + \delta_{ij}\right)\frac{\partial u'_i}{\partial x_j}$$

$$\quad (4)$$

k and ω Equations:

$$\frac{\partial}{\partial x_i}(\rho k u_i) = \frac{\partial}{\partial x_j}\left(\Gamma_k \frac{\partial k}{\partial x_j}\right) + \tilde{G}_k - Y_k + S_k \quad (5)$$

$$\frac{\partial}{\partial x_i}(\rho \omega u_i) = \frac{\partial}{\partial x_j}\left(\Gamma_\omega \frac{\partial \omega}{\partial x_j}\right) + G_\omega - Y_\omega + D_\omega + S_\omega \quad (6)$$

The constants used in the *SST k-ω* turbulence model are given below:

$$\sigma_{k,1} = 1.176, \ \sigma_{\omega,1} = 2.0, \ \sigma_{k,2} = 1.0, \ \sigma_{\omega,2} = 1.168, \ a_1 = 0.31,$$
$$\beta_{i,1} = 0.075, \ \beta_{i,2} = 0.0828, \ \alpha_\infty^* = 1.0, \ \alpha_\infty = 0.52, \ \alpha_o = 1/9,$$
$$\beta_\infty^* = 0.09, \ R_\beta = 8.0, \ R_k = 6.0, \ R_\omega = 2.95, \ \zeta^* = 1.5 \quad (7)$$

Both the domain's entrance (ABCD) and exit (EFGH) are periodic boundary conditions. Instead of assuming a constant pressure drop owing to the periodic flow condition, it is assumed that the mass flow rate of air is constant. The mass flow rate is taken corresponding to the Reynolds number in the test duct. It has been thought that the air's physical properties do not change substantially depending on the average bulk temperature. On the bottom (ABFE) and baffle surfaces, a no-slip boundary condition is used in addition to a temperature along the walls that was uniform. On both the top (DCGH) and side (BFGC) surfaces of the domain, an insulated boundary condition is used. On the symmetry plane
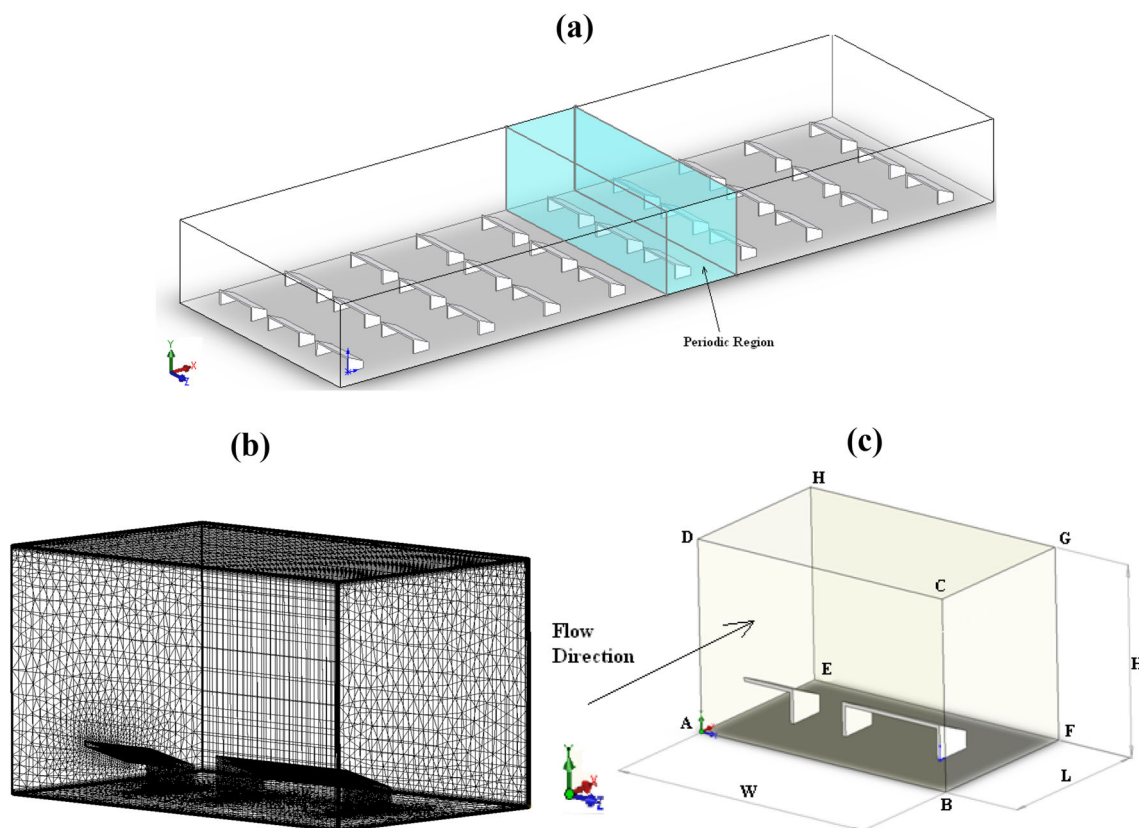
(a)

(b)

(c)

Fig. 3 **a** Appearance of the periodic region; **b** grid distribution; **c** boundary conditions of the computational domain

(AEHD), a boundary condition called symmetry is imposed. Figure 3c illustrates all of the naming that has to be done for the boundary conditions that are applied to the duct.

The computations are done using a steady segregated solver with a second-order upwind approach. In order to discretize the pressure, the standard method is used. Discretizing the pressure–velocity coupling, the SIMPLE algorithm is also implemented. It is determined that there are no issues with convergence. To achieve convergence, it is necessary to repeatedly solve each equation involving energy, momentum, mass, and turbulence until the value of the residual is reduced to a value less than 1×10^{-6}.

The grid independence investigation is carried out by reducing the size of the grid until the percentage of variance in the Darcy friction factor (f) and the Nu for each of the baffle designs is less than 1%. Figure 4 depicts the f and Nu as a function of the grid number for a baffle design of $\beta = 0.14$ rad. It is obtained that there is no big change for grid number of 210,238.

By averaging across the air flow in the duct, we can get the convective heat transfer coefficient [30]:

$$h = \frac{\dot{Q}_c}{A(T_w - T_b)} \tag{8}$$

where T_b (K) is the air bulk temperature, T_w (K) is the surface temperature, and A (m^2) is the surface area. For a duct with a rectangular cross-section, the hydraulic diameter is defined as $D_h = 4A_c/P$ where A_c (m^2) is the cross-sectional area and P (m) is the wetted perimeter. Convective heat transfer, denoted by $\dot{Q}_c$ (W), is the process by which heat is transferred from the bottom surface of the duct to the air that is passing through the duct at a constant rate of air flow. It is obtained from the equation given below:

$$\dot{Q}_c = \rho U A_c c_p (T_{bo} - T_{bi}) \tag{9}$$

where T_{bi} (K) and T_{bo} (K) are bulk temperatures at the inlet and outlet, c_p (J/kg·K) is the specific heat of the air, U (m/s) is the velocity of the air, and ρ (kg/m^3) is the density of air.

For the purposes of defining Reynolds and Nus, the hydraulic diameter is used as the defining characteristic length.

$$\text{Re} = \frac{U \cdot D_h}{v} \tag{10}$$

$$\text{Nu} = \frac{h \cdot D_h}{k} \tag{11}$$

In Eqs. (10) and (11), k (W/m K) is the thermal conductivity of air, and v (m^2/s) is the kinematic viscosity of air.

The Darcy friction factor (f) is one of the most important measurements. Conventionally, the f along the channel is written as a function of pressure drop and velocity, as shown below.

$$f = \frac{\Delta p(D_h/L)}{\rho U^2/2} \tag{12}$$

In this equation, Δp (Pa) represents the pressure drop along the duct, and L (m) represents the length of the duct.

The air thermophysical properties are taken from Bergman et al. [30].

3 Results and Discussion

This work presents the results of a numerical investigation of the fluid friction and convective heat transfer in a duct with a rectangular cross-section and flow-inclined baffles positioned on the bottom wall and subjected to a turbulent flow state. Both the f and Nu are provided as the numerical findings.

The periodic boundary condition is a good place to begin explaining the problem. Because of the periodic boundary condition, the velocity profile is the same at the domain's entrance and exit [31]. For showing the repeating of the velocity profile at the inlet–outlet of the computational domain, lines are created on the symmetry plane at the inlet–outlet of the computational domain. Variation of the velocity magnitudes with the dimensionless height of the duct (y/D_h) on these lines plotted as presented in Fig. 5a. The graphic demonstrates that the velocity profile is the same at the domain's entrance and outflow. The temperature profile of the fluid in the domain doesn't repeat itself; however, the dimensionless temperature profile, Θ, repeats itself for constant wall temperature boundary condition [30]. T_w (K) is the surface temperature of the bottom wall of the duct, and T_b (K) is the mean bulk temperature of the air flow; hence, dimensionless temperature profile is defined as $\Theta = (T(x, y, z) - T_w)/(T_b - T_w)$. It is seen in Fig. 5b, the Θ also repeats itself in the computational domain.

Figure 6a, b shows the Nu and f with changing of Reynolds number, respectively, to facilitate numerical research. Numerical results for smooth and baffled ducts can be seen in these figures. With an increase in Reynolds number, the Nu rises, while the f falls. Increasing the baffle's inclination angle is found to enhance the f and the Nu. As the inclination angle of the baffle is increased, heat transmission and friction are shown to rise significantly. As can be seen in Fig. 6a, b, the Nu and the f indicate a rising trend with an increasing baffle angle [5]. That's because the fluid's dynamic pressure is being dissipated by the act of the reverse flow and the increased surface area that results from it. The

larger the inclination angle, the more fluid is captured and sent down toward the duct's base. That's why it boosts the heat transfer rate but increases the flow resistance. In addition, the friction factor and heat transmission rate are both reduced in a smooth duct compared to a baffled duct.

Figure 6a, b show also the results of a comparison between the numerical findings and experimental data [28] found in the literature. There is a remarkable concordance between numerical and experimental findings. The f and Nu are determined to be within 6% and 8%, respectively, of the numerical values and the experimental data [28].

Finally, there is one simple empirical equation is obtained which covered the whole baffle inclination angles for Nu and f in Eqs. (13) and (14), respectively.

$$Nu = (0.0548 + 0.0521\beta)Re^{0.8} \tag{13}$$

$$f = (13.91 + 14.59\beta)Re^{-0.5} \tag{14}$$

Baffles have a substantial role in the enhancement of convective heat transfer and pressure drop. In heat exchanger design, enhancement of pressure drop is an undesirable condition. Thus, the thermal enhancement factor, η, is used to understand which characteristic (hydrodynamic or thermal) is superior. The thermal enhancement factor measures how much more efficient heat transmission is with a wall-mounted baffle compared to a flat surface [32]. If $\eta > 1$, thermal characteristics are dominant, but if $\eta < 1$, hydrodynamic characteristics are dominant. The thermal enhancement factor is obtained from Eq. (15)

$$\eta = \frac{Nu/Nu_o}{(f/f_o)^{1/3}} \tag{15}$$

where f_o and Nu_o stand for the f and Nu for the smooth duct, respectively.

Figure 7 depicts how the thermal enhancement factor changes as a function of the Reynolds number, as a result of the inclination angles of the baffles. It is clear from the graph that the Reynolds number is not a key parameter as the baffle inclination angle. The value of the thermal enhancement factor reaches the highest value for $\beta = 0.41$ rad, while it has the lowest value for $\beta = 0$ rad for all Reynolds numbers. The thermal performance of $\beta = 0.41$ rad is approximately 40% better than in case of $\beta = 0$ rad. Also, the thermal characteristics of the duct with flow-inclined baffles are more powerful compared to hydrodynamics characteristics due to $\eta > 1$.

Figure 8 displays the flow field velocity vector plot at Re = 4000 for all baffle inclination angles. The flow is seen to impinge on the duct's bottom surface as the baffle's inclination angle increases. Higher-inclination angled baffle designs also produce secondary flow fields behind them. The thermal

Fig. 4 Grid number effects on the f and Nu for the condition of $\beta = 0.14$ rad
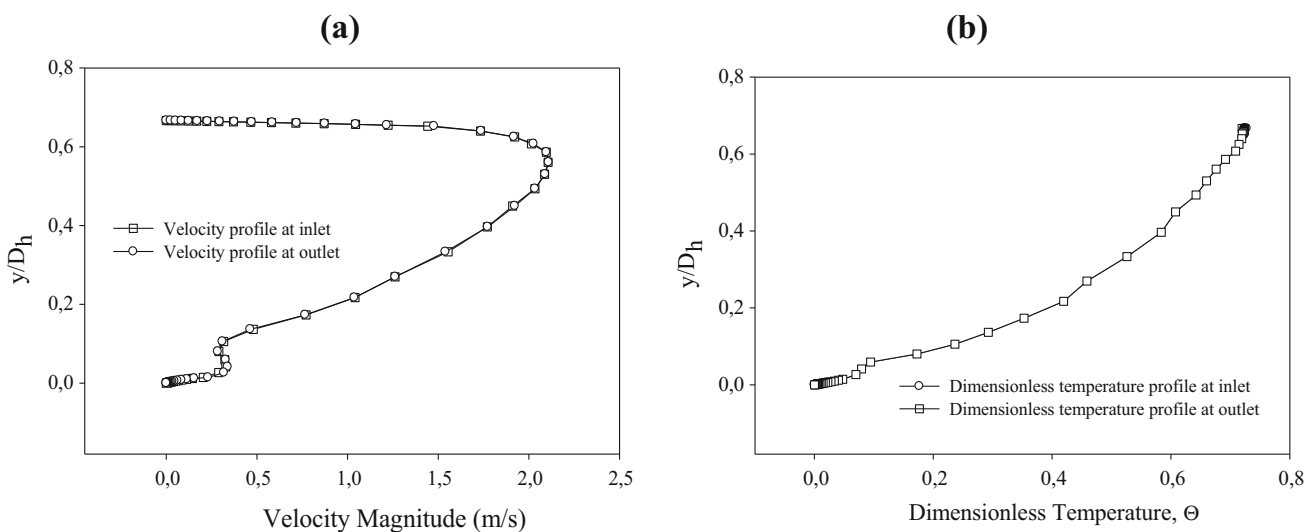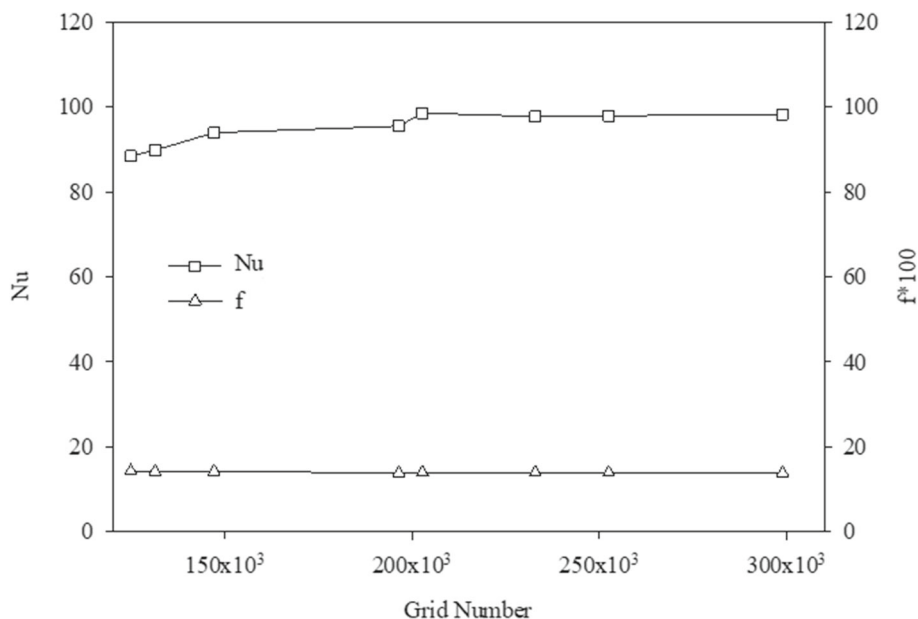

Fig. 5 The inlet and outlet velocity **a** and dimensionless temperature **b** profiles of the computational domain

boundary layer is destroyed as a result of the higher flow circulation, which causes larger turbulence intensity. These flow fields enhance the convective heat transfer [33].

The temperature contours in the duct are presented in Fig. 9 for different locations along the baffle geometry. It can be obtained that the temperature magnitudes increase near the bottom surface of the duct and the surface of the baffles. The mixing sections form at the backside of the baffles. Also, temperature magnitudes on the backside of the baffle with higher inclination angles have higher values. This condition increases the convective heat transfer. The results of the study are in agreement with [34].

4 Conclusions

Turbulent flow in a horizontal duct having rectangular cross-section with baffles inserted on the bottom surface at varied inclination degrees is analyzed computationally for fluid friction and heat transfer. The Reynolds number ranges from 1×10^3 to 1×10^4, and Pr is set to 0.7. The research presents its findings in terms of mean values for the f and the Nu. For both pressure drop and convective heat transfer, dimensionless empirical relations have been derived. The numerical findings are compared with experimental data found in the literature, and it is found that the two sets of results are consistent with one another. The findings obtained as a result of the study are listed below:

Fig. 6 Comparison of the Nu
(**a**) and f (**b**) as a function of the
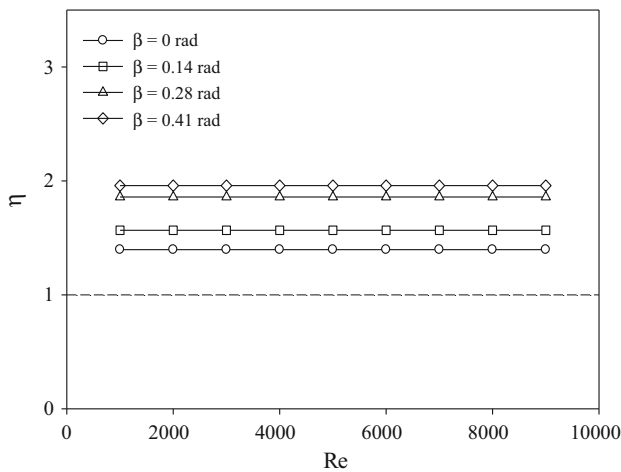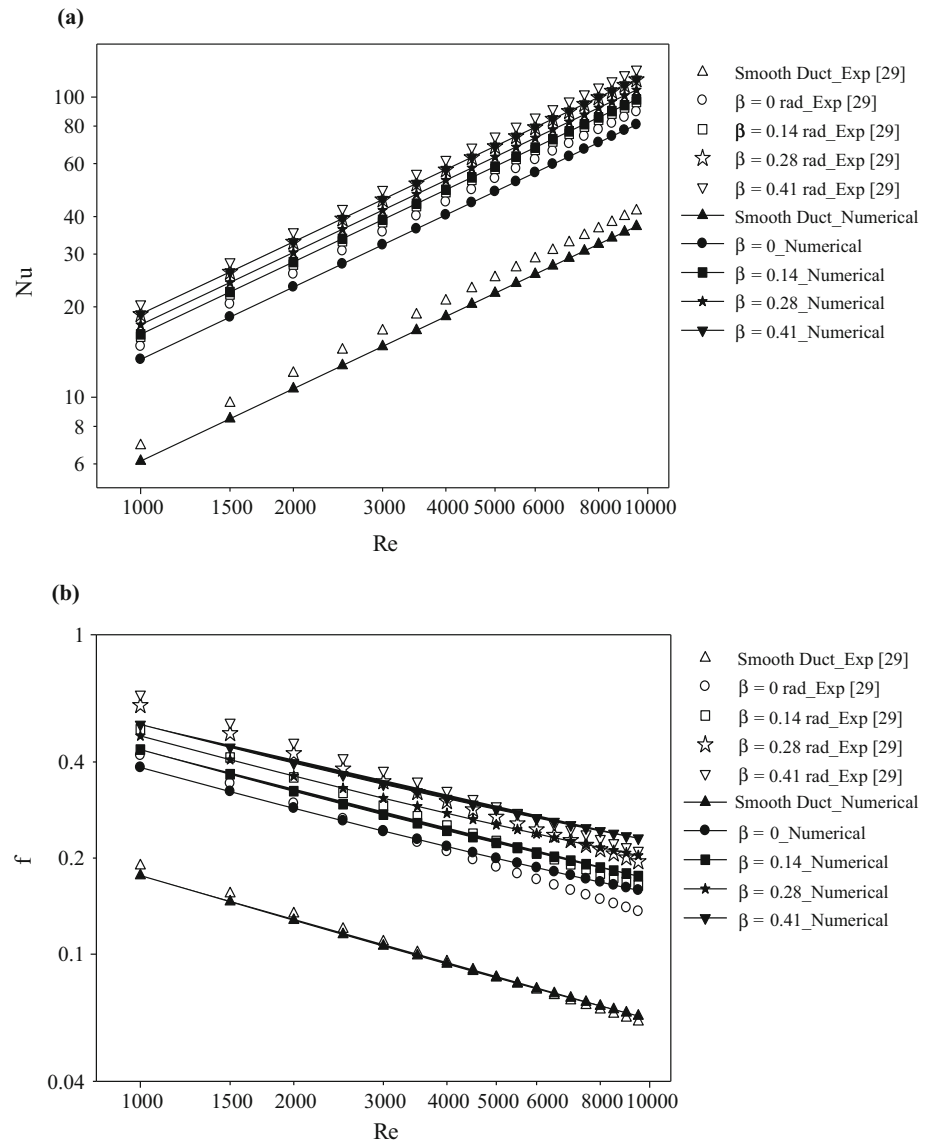Reynolds number with Ref [28]

(a)

- Smooth Duct_Exp [29]
- β = 0 rad_Exp [29]
- β = 0.14 rad_Exp [29]
- β = 0.28 rad_Exp [29]
- β = 0.41 rad_Exp [29]
- Smooth Duct_Numerical
- β = 0_Numerical
- β = 0.14_Numerical
- β = 0.28_Numerical
- β = 0.41_Numerical

(b)

- Smooth Duct_Exp [29]
- β = 0 rad_Exp [29]
- β = 0.14 rad_Exp [29]
- β = 0.28 rad_Exp [29]
- β = 0.41 rad_Exp [29]
- Smooth Duct_Numerical
- β = 0_Numerical
- β = 0.14_Numerical
- β = 0.28_Numerical
- β = 0.41_Numerical

- β = 0 rad
- β = 0.14 rad
- β = 0.28 rad
- β = 0.41 rad

- Nu increases with increasing flow rate for all cases.
- Increasing the Reynolds number results in a reduction in the f inside the duct.
- f and Nu increase with increasing the baffle inclination angle.
- The findings of the numerical solutions reveal a relationship between the f and the Reynolds number across all of the baffle inclination degrees. Also, the same type of relationship is seen for the Nu and the Reynolds number.
- Empirical relations are derived for variation of Nu and f with Reynolds number and baffle inclination angle.
- It is obtained that the thermal enhancement factor is greatest for the $\beta = 0.41$ rad baffle inclination angle when compared to the other baffle inclination angles.
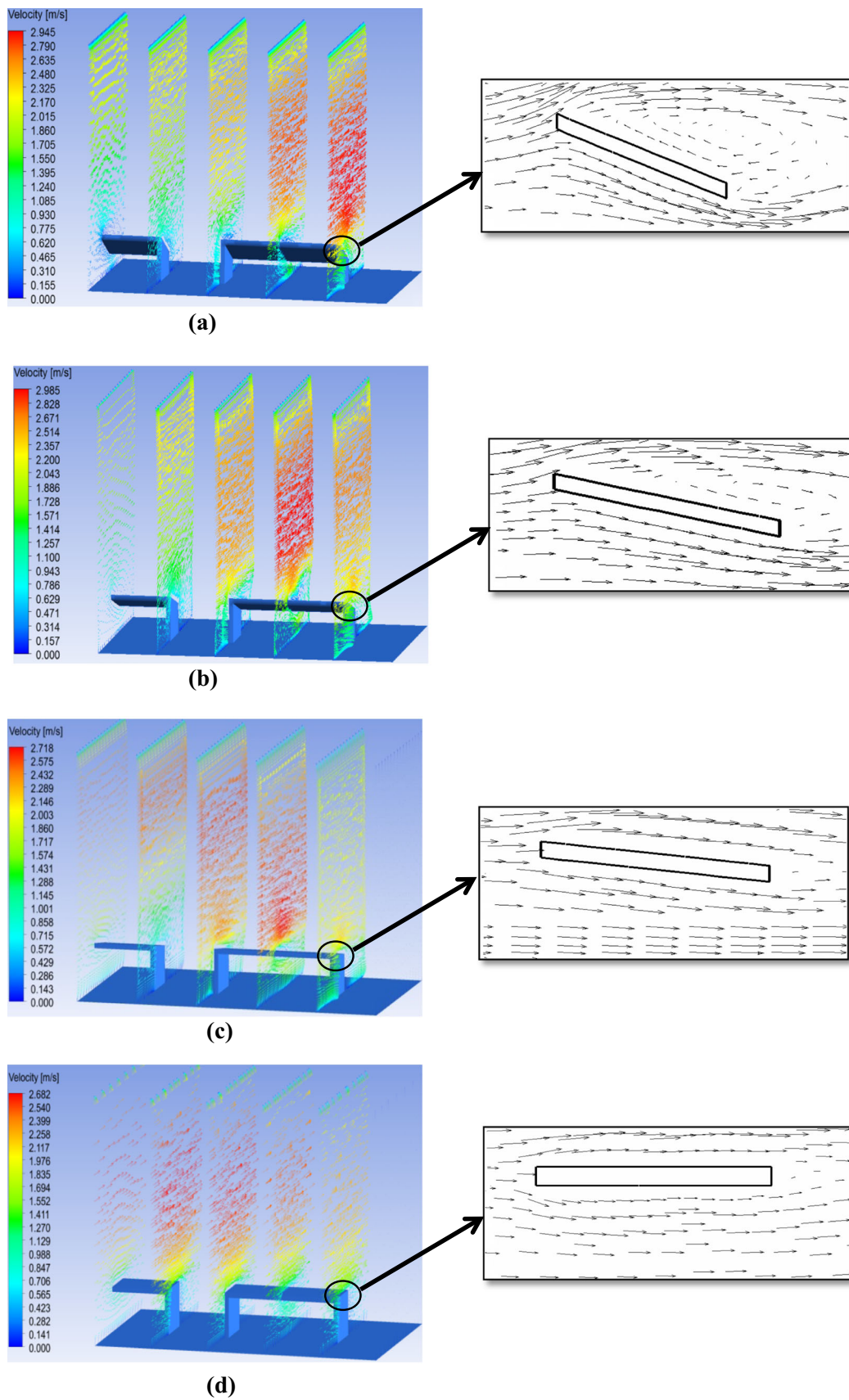
Fig. 7 Variation of thermal enhancement factor with Reynolds number
for different baffle inclination angles

Fig. 8 The vector plots of velocity; **a** $\beta = 0.41$ rad, **b** $\beta = 0.28$ rad, **c** $\beta = 0.14$ rad, **d** $\beta = 0$ rad
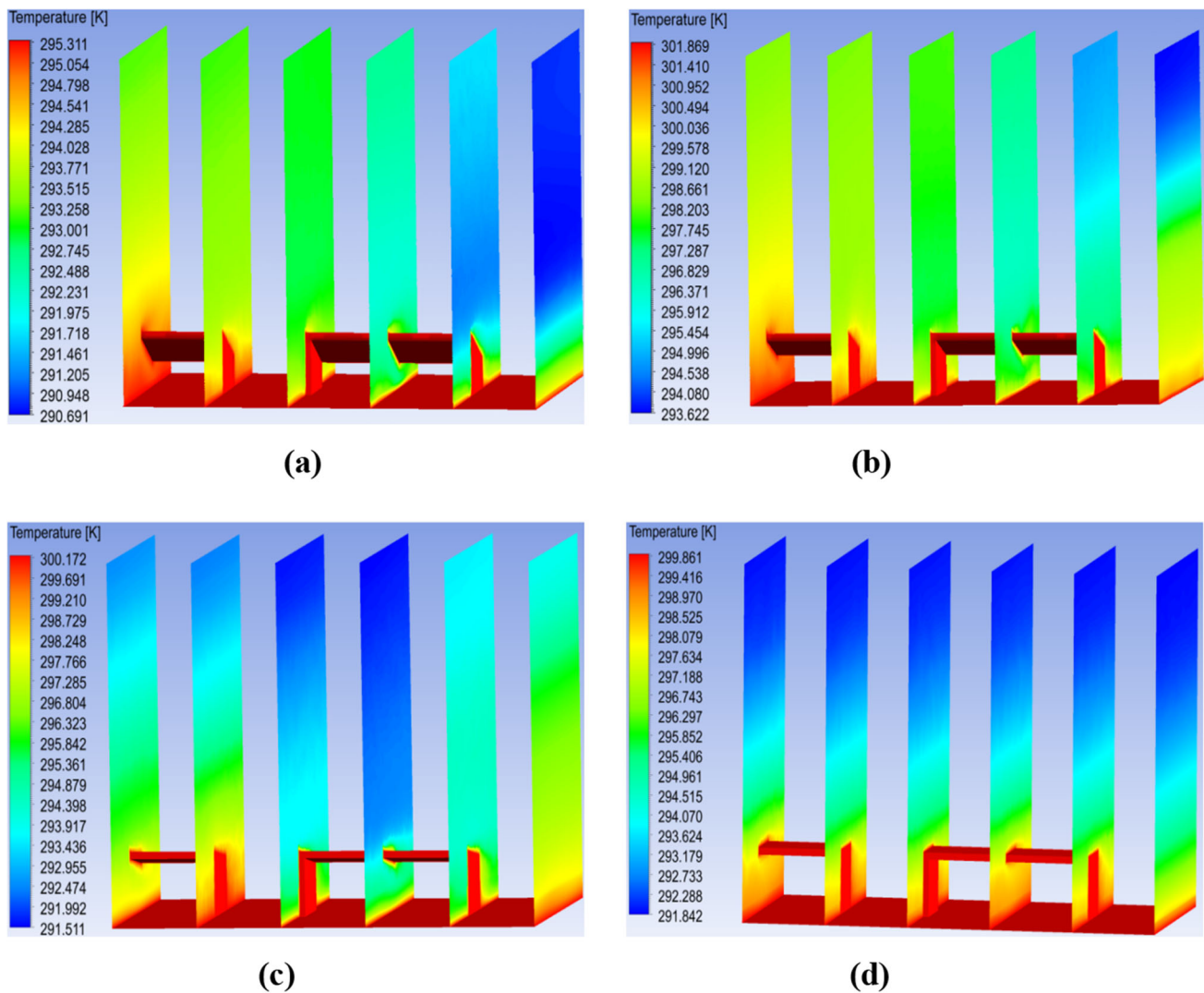
Fig. 9 Contour plots of temperature; **a** $\beta = 0.41$ rad, **b** $\beta = 0.28$ rad, **c** $\beta = 0.14$ rad, **d** $\beta = 0$ rad

References

1. Dutta, P.; Dutta, S.: Effect of baffle size, perforation, and orientation on internal heat transfer enhancement. Int. J. Heat Mass Transf. **41**, 3005–3013 (1998). https://doi.org/10.1016/S0017-9310(98)00016-7

2. Salem, M.R.; Althafeeri, M.K.; Elshazly, K.M.; Higazy, M.G.; Abdrabbo, M.F.: Experimental investigation on the thermal performance of a double pipe heat exchanger with segmental perforated baffles. Int. J. Therm. Sci. **122**, 39–52 (2017). https://doi.org/10.1016/j.ijthermalsci.2017.08.008

3. Kumar, R.; Kumar, A.; Sharma, A.; Chauhan, R.; Sethi, M.: Experimental study of heat transfer enhancement in a rectangular duct distributed by multi V-perforated baffle of different relative baffle width. Heat Mass Transf. **53**, 1289–1304 (2017). https://doi.org/10.1007/s00231-016-1901-7

4. Eiamsa-ard, S.; Chuwattanakul, V.: Visualization of heat transfer characteristics using thermochromic liquid crystal temperature measurements in channels with inclined and transverse twisted-baffles. Int. J. Therm. Sci. **153**, 106358 (2020). https://doi.org/10.1016/j.ijthermalsci.2020.106358

5. Skullong, S.; Thianpong, C.; Jayranaiwachira, N.; Promvonge, P.: Experimental and numerical heat transfer investigation in turbulent square-duct flow through oblique horseshoe baffles. Chem. Eng. Process. Process Intensif. **99**, 58–71 (2016). https://doi.org/10.1016/j.cep.2015.11.008

6. Qayoum, A.; Panigrahi, P.: Experimental investigation of heat transfer enhancement in a two-pass square duct by permeable ribs. Heat Transf. Eng. **0**, 1–12 (2018). https://doi.org/10.1080/01457632.2018.1436649

7. Wang, D.; Wang, H.; Xing, J.; Wang, Y.: Investigation of the thermal-hydraulic characteristics in the shell side of heat exchanger with quatrefoil perforated plate. Int. J. Therm. Sci. **159**, 106580 (2021). https://doi.org/10.1016/j.ijthermalsci.2020.106580

8. Ko, K.-H.; Anand, N.K.: Use of porous baffles to enhance heat transfer in a rectangular channel. Int. J. Heat Mass

Transf. **46**, 4191–4199 (2003). https://doi.org/10.1016/S0017-9310(03)00251-5

9. Jedsadaratanachai, W.; Jayranaiwachira, N.; Promvonge, P.: 3D numerical study on flow structure and heat transfer in a circular tube with V-baffles. Chin. J. Chem. Eng. **23**, 342–349 (2015). https://doi.org/10.1016/j.cjche.2014.11.006

10. Promvonge, P.: Thermal performance in square-duct heat exchanger with quadruple V-finned twisted tapes. Appl. Therm. Eng. **91**, 298–307 (2015). https://doi.org/10.1016/j.applthermaleng.2015.08.047

11. Sripattanapipat, S.; Promvonge, P.: Numerical analysis of laminar heat transfer in a channel with diamond-shaped baffles. Int. Commun. Heat Mass Transf. **36**, 32–38 (2009). https://doi.org/10.1016/j.icheatmasstransfer.2008.09.008

12. Menni, Y.; Azzi, A.; Zidani, C.: Use of waisted triangular-shaped baffles to enhance heat transfer in a constant temperature- surfaced rectangular channel. J. Eng. Sci. Technol. **12**, 23 (2017)

13. Thermal performance assessment of turbulent channel flows over different shaped ribs—ScienceDirect. https://www.sciencedirect.com/science/article/pii/S0735193308001620

14. Kelkar, K.M.; Patankar, S.V.: Numerical prediction of flow and heat transfer in a parallel plate channel with staggered fins. J. Heat Transf. **109**, 25–30 (1987). https://doi.org/10.1115/1.3248058

15. Kamali, R.; Binesh, A.R.: The importance of rib shape effects on the local heat transfer and flow friction characteristics of square ducts with ribbed internal surfaces. Int. Commun. Heat Mass Transf. **35**, 1032–1040 (2008). https://doi.org/10.1016/j.icheatmasstransfer.2008.04.012

16. Fawaz, H.E.; Badawy, M.T.S.; Abd Rabbo, M.F.; Elfeky, A.: Numerical investigation of fully developed periodic turbulent flow in a square channel fitted with 45° in-line V-baffle turbulators pointing upstream. Alex Eng J **57**, 633–642 (2018). https://doi.org/10.1016/j.aej.2017.02.020

17. Debnath, P.; Pradhan, M.: A recent state of art review on heat transfer enhanced characteristics and material selection of SCTHX. Proc. Inst. Mech. Eng. Part E J. Process. Mech. Eng. **1**, 2 (2022). https://doi.org/10.1177/09544089221124463

18. Masud, S.; Roy, N.C.; Saha, L.K.: Thermal decomposition of a reacting chemical in a stepped rectangular channel with multiple obstacles. Alex. Eng. J. **61**, 10743–10755 (2022). https://doi.org/10.1016/j.aej.2022.04.016

19. Ibrahim, M.; Algehyne, E.A.; Saeed, T.; Berrouk, A.S.; Chu, Y.-M.; Cheraghian, G.: Assessment of economic, thermal and hydraulic performances a corrugated helical heat exchanger filled with non-Newtonian nanofluid. Sci. Rep. **11**, 11568 (2021). https://doi.org/10.1038/s41598-021-90953-6

20. Ibrahim, M.; Saeed, T.; Bani, F.R.; Sedeh, S.N.; Chu, Y.-M.; Toghraie, D.: Two-phase analysis of heat transfer and entropy generation of water-based magnetite nanofluid flow in a circular microtube with twisted porous blocks under a uniform magnetic field. Powder Technol. **384**, 522–541 (2021). https://doi.org/10.1016/j.powtec.2021.01.077

21. Promvonge, P.; Koolnapadol, N.; Pimsarn, M.; Thianpong, C.: Thermal performance enhancement in a heat exchanger tube fitted with inclined vortex rings. Appl. Therm. Eng. **62**, 285–292 (2014). https://doi.org/10.1016/j.applthermaleng.2013.09.031

22. Lu, B.; Jiang, P.-X.: Experimental and numerical investigation of convection heat transfer in a rectangular channel with angled ribs. Exp. Therm. Fluid Sci. **30**, 513–521 (2006). https://doi.org/10.1016/j.expthermflusci.2005.09.007

23. Akbari, O.A.; Toghraie, D.; Karimipour, A.; Safaei, M.R.; Goodarzi, M.; Alipour, H.; Dahari, M.: Investigation of rib's height effect on heat transfer and flow parameters of laminar water–Al$_2$O$_3$ nanofluid in a rib-microchannel. Appl. Math. Comput. **290**, 135–153 (2016). https://doi.org/10.1016/j.amc.2016.05.053

24. Pourfattah, F.; Motamedian, M.; Sheikhzadeh, G.; Toghraie, D.; Ali Akbari, O.: The numerical investigation of angle of attack of inclined rectangular rib on the turbulent heat transfer of Water-Al$_2$O$_3$ nanofluid in a tube. Int. J. Mech. Sci. **131–132**, 1106–1116 (2017). https://doi.org/10.1016/j.ijmecsci.2017.07.049

25. Roy, N.C.: Unsteady behaviors of natural convection flow of a reactant in a thin finned enclosure. Phys. Fluids. **33**, 083616 (2021). https://doi.org/10.1063/5.0059828

26. Roy, N.C.: Augmentation in heat transfer for a hybrid nanofluid flow over a roughened surface. Case Stud. Therm. Eng. **27**, 101215 (2021). https://doi.org/10.1016/j.csite.2021.101215

27. Sparrow, E.M.; Tao, W.Q.: Symmetric vs asymmetric periodic disturbances at the walls of a heated flow passage. Int. J. Heat Mass Transf. **27**, 2133–2144 (1984). https://doi.org/10.1016/0017-9310(84)90200-X

28. Arslan, K.; Onur, N.: Experimental investigation of flow and heat transfer in rectangular cross-sectioned duct with baffles mounted on the bottom surface with different inclination angles. Heat Mass Transf. **50**, 169–181 (2014). https://doi.org/10.1007/s00231-013-1236-6

29. ANSYS Fluent Theory Guide. Fluent Corporation, Lebanon, New Hampshire (2006)

30. Bergman, T.L.; Incropera, F.P.; DeWitt, D.P.; Lavine, A.S.: Fundamentals of Heat and Mass Transfer. Wiley, New York (2011)

31. Patankar, S.V.; Liu, C.H.; Sparrow, E.M.: Fully developed flow and heat transfer in ducts having streamwise-periodic variations of cross-sectional area. J. Heat Transf. **99**, 180–186 (1977). https://doi.org/10.1115/1.3450666

32. Thianpong, C.; Chompookham, T.; Skullong, S.; Promvonge, P.: Thermal characterization of turbulent flow in a channel with isosceles triangular ribs. Int. Commun. Heat Mass Transf. **36**, 712–717 (2009). https://doi.org/10.1016/j.icheatmasstransfer.2009.03.027

33. Menni, Y.; Chamkha, A.J.; Makinde, O.D.: Turbulent heat transfer characteristics of a w-baffled channel flow—heat transfer aspect. Defect Diffus. Forum. **401**, 117–130 (2020). https://doi.org/10.4028/www.scientific.net/DDF.401.117

34. Sahel, D.: Thermal performance assessment of a tubular heat exchanger fitted with flower baffles. J. Thermophys. Heat Transf. **35**, 726–734 (2021). https://doi.org/10.2514/1.T6208